Water Air Soil Pollut (2020) 231:192
https://doi.org/10.1007/s11270-020-04557-3

Removal of Organic Pollutants from Effluent of Anaerobic Digester Using Hydrochars Produced from Faecal Simulant and Sewage Sludge

Eric Danso-Boateng · Eleni Nyktari · Andrew D. Wheatley · Richard G. Holdich · Abubakar S. Mohammed

Received: 4 February 2020 / Accepted: 26 March 2020

Abstract Hydrochars produced from hydrothermal carbonisation of faecal simulant (FS) at 180 °C for 30 min and sewage sludge treated via CAMBI process at 165 °C for 30 min were used for adsorption of organic pollutants in effluent from an anaerobic digester (AD). The adsorption potential of the hydrochars investigated was compared with that of a commercial powdered activated carbon (PAC). It was found that the CAMBI and FS hydrochars were effective only after chemical activation. KOH activation increased chemical oxygen demand (COD) removal from 33.0 to 59.6% and 75.2% for FS and CAMBI, respectively. Extra activation with HCl improved the adsorption efficiency of FS, increasing COD removal to 79.3%, but not for the CAMBI hydrochar even though its surface area was increased. Acidic pH aided organics removal for both hydrochars. PAC adsorption capacity was the highest (> 90%), and this was not affected by pH. All the adsorbents could successfully remove the organics in a very short time as 30 min. The optimum dosage of the hydrochars to reach a high uptake of organics was 30.0 g/L. The adsorption reaction followed a pseudo-second-order kinetic model for all the hydrochars. The adsorption onto the hydrochars correlated well with Temkin isotherm model and followed a type II and IV isotherm type, except PAC which was described by the Langmuir isotherm with a high adsorption capacity of 400.0 mg/g. The study demonstrated that hydrochars of FS and CAMBI activated with KOH are efficient and sustainable adsorbents for the removal of organics from AD effluent.

Keywords Adsorption · Anaerobic digestion · Biomass · Hydrochar · Hydrothermal carbonisation

E. Danso-Boateng (✉)
School of Chemical and Process Engineering, University of Leeds, Leeds LS2 9JT, UK
e-mail: e.danso-boateng@leeds.ac.uk

E. Nyktari · R. G. Holdich
Department of Chemical Engineering, Loughborough University, Loughborough LE11 3TU, UK

A. D. Wheatley · A. S. Mohammed
School of Architecture, Building and Civil Engineering, Loughborough University, Loughborough LE11 3TU, UK

1 Introduction

Anaerobic digestion (AD) of hydrothermal wastewater or liquid by-products following hydrothermal carbonisation (HTC) of biomass has gain research interest in recent times (Wirth and Mumme 2013; Danso-Boateng et al. 2015; Wirth et al. 2015; Nyktari et al. 2017; de La Rubia et al. 2018; Weide et al. 2019). Studies have shown that the hydrothermal wastewater can contain high chemical oxygen demands (CODs) ranging from 10.0 to 40.0 g/L, total organic carbon (TOC) contents of 5.0–40.0 g/L, and depending on the feedstock used and the HTC process conditions, carboxylic acids, sugars, phenols, polycyclic aromatic hydrocarbons and Maillard products such as aldehydes, furans, pyrroles, pyrazines and pyridines (Wirth et al. 2012; Danso-Boateng et al. 2015). Hence, to minimise environmental pollution (Nelson et al. 2013) and to

Published online: 18 April 2020

enhance the energy budget of the HTC process, anaerobic digestion of the hydrothermal wastewater to produce biogas (Danso-Boateng et al. 2015; Tommaso et al. 2015) is a needed.

It has been reported that AD could reduce COD of the hydrothermal wastewater by 20.0–61.0% (Chen et al. 2016; Nyktari et al. 2017), with continuous digestion using continuous stirred-tank reactors (CSTR) resulting in COD degradation rates of 52.0–68.0% (Wirth et al. 2012; Wirth et al. 2015; Fernandez et al. 2018; Weide et al. 2019). However, previous studies show that COD contents in the digester final effluent following AD are still high, with levels between 4.5 and 11.8 g/L (Nyktari et al. 2017), indicating the need for further treatment before being discharged into the environment.

Several methods for the treatment of wastewater exist, namely the use of activated carbons, chemical coagulation/flocculation, oxidation, electrochemical and membrane techniques. However, the removal of organic compounds from aqueous streams by activated carbon via adsorption has been widely studied as the other methods have several disadvantages which limit their applications. For instance, adsorption of malachite green dye by activated carbon derived from a jackfruit peel (Ibaraj and Sulochana 2002); methylene blue by activated carbon derived from a Malaysian bamboo (Hameed et al. 2007); COD removal using activated carbon derived from a Nigerian-based bamboo (Ademiluyi et al. 2009); adsorption of dibromochloropropane from well waters by almond shell–derived activated carbon (Klasson et al. 2013); and removal of catechol and resorcinol from aqueous solution using activated carbon derived from sunflower seed hull residues (Vunain et al. 2018). However, activated carbons requires extremely high processing temperatures (> 800 °C), which makes it expensive for use as adsorbents, particularly in developing countries.

Besides activated carbons, adsorption of dyes from wastewater using biochars derived from straw and bamboo has been reported (Hameed and El-Khaiary 2008; Mui et al. 2010; Xu et al. 2011; Yang et al. 2014). Adsorption of phenols by biochars derived from rice husk, corncob and food waste (Liu et al. 2011; Lee et al. 2019) and adsorption of COD using nanotube-biochar nanocomposites (Inyang et al. 2014) have been reported. However, like activated carbons, biochar requires high processing temperature (350–900 °C). This therefore limits their large-scale application due to the high costs (Alatalo et al. 2013; Ramavandi and Farjadfard 2014).

Research in recent times has been focusing on substitutes of biochar and activated carbon (Mohan et al. 2014), with a particular interest in HTC. In contrast to conventional pyrolysis to produce biochar, HTC requires moderate processing temperatures (typically, 180–250 °C) (Funke and Ziegler 2010). Depending on the applied process conditions, carbon recovery in the final carbonised solids (called 'hydrochar') can be very high (Titirici and Antonietti 2010; Parshetti et al. 2013; Danso-Boateng et al. 2015). Also, hydrochars and biochars have different chemical structures because of the different processing conditions applied in both methods (Cao et al. 2010; Titirici and Antonietti 2010; Titirici et al. 2012). Sun et al. (2011) reported that biochars and hydrochars have different sorption abilities due to the differences in their chemical composition, physical structures and polarity.

A few studies have reported the use of hydrochars for the removal of organic contaminants from aqueous solutions. Hydrochars derived from activated sludge have been reported as adsorbents for the removal of dye (Crini 2006) and pathogens (Chung et al. 2015; Chung et al. 2017) in wastewater. Sun et al. (2011) investigated adsorption of bisphenol A, 17a-ethinyl estradiol and phenanthrene by hydrochars derived from swine solids and poultry litter and found that both adsorbents exhibited higher sorption capacity than biochars derived from the same materials at 400 °C. However, the potential mechanism underlying the sorption capacity of the hydrochars was not studied in their work. Unlike organic contaminants, more studies have reported the adsorption of heavy metals by hydrochars derived from different materials (Inyang et al. 2012; Lu et al. 2012; Chung et al. 2015; Fang et al. 2015; Koottatep et al. 2017). However, unlike heavy metals adsorption, studies into the application of hydrochars for removal of organic contaminants are in developing stages.

The limited information on the exact mechanism of adsorption of organic pollutants onto hydrochars makes it essential to conduct further research in this area. Also, most of the studies centred on the removal of certain contaminants from synthetic wastewater. Real wastewater is more complex and contains several different organic compounds (Tan et al. 2015). Particularly, the composition of HTC wastewater is very complex (Danso-Boateng et al. 2015) as a result of the organic compounds generated during the HTC process. Also,

unlike lignocellulosic biomass, sewage sludge is very complex consisting of carbohydrate (fibre), protein, fat and inorganics (nitrogen, minerals and phosphorus) (Yakovlev and Voronov 2002). Hence, sorption characteristics of sewage sludge–derived hydrochars will differ from those of lignocellulosic biomass.

So far, studies into the circularity of the HTC process are not yet available in literature. A complete process of HTC-AD followed by adsorption using the same solids (hydrochar) from the basic process to ensure that no harmful waste is being discharged to the environment will promote economic circularity. This would render sewage sludge treatment via integrated HTC-AD-adsorption, a sustainable and green technology, especially for developing countries.

This study therefore investigates the sorption capacity of hydrochars produced from faecal simulant and sewage sludge. There is limited information in literature examining the potential of hydrochars of sewage/faecal sludge for removal of organic contaminants in HTC wastewater and/or effluents of wastewater following anaerobic digestion of HTC liquid by-products. Therefore, the specific objectives of this study are to investigate the (i) potential of sewage and faecal sludge hydrochars in removing organic pollutants, represented by COD and TOC; (ii) effect of pH on adsorption capacity/efficiency; (iii) effect of retention time on adsorption efficiency; (iv) effect of adsorbent dosage on adsorption efficiency; (v) effect of chemical activation on adsorption efficiency and (vi) the mechanisms accounting for their sorption capacity. To understand the physicochemical properties of the hydrochars, they will be characterised using scanning electron microscopy (SEM), surface area and pore size distribution, and Fourier transform infrared (FTIR) spectrometry.

2 Materials and Methods

2.1 Adsorbents and Wastewater

Powdered activated charcoal (PAC) 4-8 mesh used as a benchmark was supplied by Sigma-Aldrich, USA. It was an untreated, granular carbon with a particle size of 2.4–4.6 mm and BET surface area of 993 m^2/g.

Thermally treated sewage sludge following the CAMBI process was collected from Anglian Water plant (Milton Keynes, UK). The process followed in the CAMBI process is hydrothermal treatment (HT) of activated sludge at 165 °C for 30 min before AD. The CAMBI sludge was collected after HT but before the AD stage. The HT CAMBI sludge was filtered through a 125-μm sieve by gravity, rinsed with methanol to remove any organics, then rinsed again with deionised water to remove the methanol and finally dried at 105 °C for 24 h to obtain the CAMBI hydrochar.

Faecal simulant (FS) was produced by following the recipe by Wignarajah et al. (2006), which contained cellulose (37.5%), yeast (37.5%), peanut oil (20.0%), KCl (4%), $Ca(H_2PO_4)_2$ (1.0%) (all purchased from Sigma-Aldrich, UK) and tap water—which constituted 90% (wt) of the FS. The FS hydrochar was produced by HTC of the FS-water mixture at 180 °C for 30 min using a 5-L capacity internally designed hydrothermal reactor. After HTC, the carbonised solids were filtered through a 60-μm sieve to obtain the hydrochar. Similarly, the FS hydrochar was further rinsed with methanol, followed by deionised water, and finally, dried at 105 °C for 24 h.

The wastewater was an effluent from a previous work on AD of the liquid by-product following HTC of FS (Nyktari et al. 2017).

2.2 Chemical Activation

The purpose of the KOH activation was to enhance the adsorption capacity of the hydrochars. This was done by soaking each hydrochar in a 1.0 M KOH solution at a temperature of 60–70 °C, and then stirred for 1 h. After this, it was rinsed with deionised water until the pH became neutral and dried at 105 °C overnight. The resulting adsorbents are termed, 'FS + KOH' and 'CAMBI + KOH'. An extra HCl activation was carried out after the KOH activation to remove the inorganics by following the same steps as in the KOH activation, producing FS + KOH + HCl and CAMBI + KOH + HCl hydrochars. All the hydrochars after the treatments were stored in a cold room at 4 °C.

2.3 Material Characterisation

2.3.1 Surface Area and Pore Size Distribution

The surface area and pore size distribution of the hydrochars were analysed using a surface area and porosity analyser (TriStar 3000, Micrometrics Instrument Corporation, USA). The samples were initially outgassed under dynamic vacuum at 110 °C to remove any residual water and organics. The samples were

analysed under liquid N_2 as the adsorbing gas at − 196 °C (77 K) in regulated amounts. The quantity adsorbed was automatically analysed using the multi-point Brunauer-Emmett-Teller (BET) method. The Barrett-Joyner-Halenda (BJH) adsorption-desorption isotherm method (Barrett et al. 1951) was used to determine the pore size distribution.

2.3.2 FTIR Spectroscopy Analysis

The functional groups in the hydrochars were analysed using a FTIR spectrometer (Nicolet 6700, Thermo Fisher Scientific, USA) at a wavenumber between 4000 and 500 cm^{-1} using 16 scans. A few grams of the dry hydrochars were placed on the platform and compressed to ensure that the sample was in good contact with the attenuated total reflectance crystal. To check the cleanliness of the sample platform, a blank was initially examined by wiping the sample platform and analysing without placing any sample on it. This step was repeated before the analysis of each sample was conducted.

2.3.3 SEM Analysis

The morphology of the hydrochars was examined using a field emission gun SEM analyser (LEO 1530 VP FEG-SEM, Carl Zeiss, Germany), which was operated at 5.0 kV, 15 mA and 20 mTorr for 5 min. Before the SEM analysis, each hydrochar sample was fitted on a 12.5-mm aluminium stub using conductive adhesive carbon tabs, and then sputter coated with gold/palladium to produce a 5.0–10.0-nm conductive layer. The working distance was set between 15.00 and 18.50 mm. The SEM images of the hydrochars were analysed at different magnifications such as × 100, × 250, × 1000 and × 2000; and the clearer images were further examined.

2.4 Adsorption Experiments

Adsorption experiments were conducted by using an adsorbent dose of 3.0 g per 100.0 mL of wastewater for all experiments, apart from isotherm study. Each hydrochar (3.0 g) and the wastewater (100 mL) were put in a 250-mL conical flask and placed in a mechanical shaker (Gallenkamp Orbital Incubator-cooled Shaker, INR-200 INR-250, Netherlands). The samples were then mixed at a constant speed of 150 rpm at a room temperature (21 ± 1 °C) for the required contact times, which ranged from 10 to 1440 min.

At the end of each experiment, the wastewater-adsorbent mixture was centrifuged at 1000 rpm for 10 min using an Eppendorf centrifuge (Eppendorf 5804, Hamburg, Germany), and the supernatant solution was collected for analysis of COD and TOC concentrations (see section 2.4.1 COD and TOC Analysis).

To investigate the effect of pH on the adsorption capacity of the hydrochars, experiments were conducted at pH of 2, 5 and 9, by using 1.0 M HCl or NaOH solutions to adjust the pH to the desired values. The same adsorbent dose of 30.0 g/L of wastewater was used. After adsorption, samples were taken at different contact times, and the COD and TOC concentrations of the effluent were analysed as explained in section 2.4.1. COD and TOC Analysis.

The effect of adsorbent dosage on adsorption efficiency was investigated by varying the adsorbent dose in range 1.0–70.0 g/L by maintaining the natural pH of the hydrochars.

2.4.1 COD and TOC Analysis

Total and soluble COD of the effluents following adsorption were analysed using a COD Analyser (Palintest 2000 and 20,000 mg/L, Palintest Ltd., UK) according to the procedure of Standard Methods 5220 D. TOC was determined using a TOC Analyser (DC-190, Rosemount Dohrmann, USA) as described by Standard Methods 5310 B. When necessary, the effluent of the adsorption experiments was diluted by ratio of 1:10. All analyses were done in triplicates.

2.4.2 Adsorption Capacity

COD and TOC removal efficiency were calculated by using Eq. (1) below.

$$\text{Removal efficiency}\ (\%) = \frac{(C_0 - C_e)}{C_0} \times 100 \qquad (1)$$

where C_0 is the initial COD or TOC concentration (mg/L) and C_e is the equilibrium COD or TOC concentration (mg/L).

The TOC or COD uptake per gram of sorbent was determined as follows:

$$q_e = \frac{(C_0 - C_e)}{m} \times V \qquad (2)$$

where q_e is the equilibrium adsorption capacity (mg/g), m is the dry weight of the adsorbent (g) and V is the volume of wastewater.

2.4.3 Adsorption Kinetics

The following kinetic models, in linear forms, were used in this study:

Pseudo-first-order model:

$$\log(q_e - q_t) = \log q_e - k_1 t \quad (3)$$

Pseudo-second-order model:

$$\frac{t}{q_t} = \frac{1}{(k_2 . q_e^2)} + \frac{t}{q_e} \quad (4)$$

Intraparticle diffusion model:

$$q_t = k_3 t^{1/2} + C \quad (5)$$

Elovich model:

$$q_t = \frac{1}{\beta}\ln(\alpha\beta) + \frac{1}{\beta}\ln(t) \quad (6)$$

where $q_t$is the amount of TOC adsorbed at time t (mg/g), and k_1 (min^{-1}) and k_2 (g/mg min) are the pseudo-first-order and pseudo-second-order adsorption rate constants respectively, k_3 (mg/g $min^{1/2}$) is the intraparticle diffusion rate constant, α (mg/g min) is the initial adsorption rate and β (g/mg) is the adsorption constant. In Eq. (3), a plot of $\ln(q_e - q_t)$ vs. t should yield a slope of $-k_1$ and an intercept of $\ln(q_e)$. In Eq. (4), a plot of t/q_t vs. t should give a slope of $1/q_e$ and an intercept of $1/(k. q_e^2)$, whilst Eq. (5) should yield a slope of k_3 and an intercept of C. A plot of q_t vs. $\ln(t)$ in Eq. (6) should produce a slope of $1/\beta$ and an intercept of $1/\beta \ln(\alpha\beta)$.

2.4.4 Adsorption Isotherms

The adsorption mechanism was investigated by using the isotherms below.

Freundlich isotherm:

$$q_e = K_F C_e^{\,1/n} \quad (7)$$

$$\log q_e = \log K_F + \left(1/n\right)\log C_e \quad (8)$$

where K_F is the relative adsorption capacity of the adsorbent (mg/g) and n is a constant related to adsorption intensity. The sorption data were analysed using the linear form of the model (Eq. 8).

Langmuir isotherm:

$$q_e = \frac{b\, q_m\, C_e}{1 + b\, C_e} \quad (9)$$

$$\frac{1}{q_e} = \frac{1}{bq_m} \cdot \frac{1}{C_e} + \frac{1}{q_m} \quad (10)$$

where q_m is the complete monolayer on the surface bound at high C_e (mg/g) and b is the Langmuir constant (L/mg). The sorption data was analysed according to the linear form of the model (Eq. 10).

Temkin model:

$$q_e = \frac{RT}{b_T}\ln(A_T C_e) \quad (11)$$

$$q_e = \frac{RT}{b_T}\ln A_T + \left(\frac{RT}{b_T}\right)\ln C_e \quad (12)$$

where R is the universal gas constant (8.31441 J/mol K), T is the absolute temperature (K), A_T is the Temkin isotherm constant (g/mg) and b_T is the Temkin constant. The linear form of the Temkin isotherm (Eq. 12) was used to analyse the sorption data.

3 Results and Discussion

3.1 Surface Morphology

SEM images of the hydrochars are shown in Figs. 1 and 2. The SEM images of CAMBI hydrochars (Fig. 1) show rougher surfaces than those of FS hydrochars (Fig. 2), which may be due to the comparably complex composition of the actual (CAMBI) sludge. As shown in Fig. 1b, c, e, f, the KOH and HCl activation of the CAMBI hydrochar resulted in the production of thinner fibres. For the FS hydrochar, the KOH activation smoothened the surface (Fig. 2b, e), which is more evident with the additional HCl treatment shown in Fig. 2c, f.

3.2 Specific Surface and Pore Size Distribution

Table 1 shows the results of BET surface area, total pore volume and BJH adsorption/desorption pore diameter of

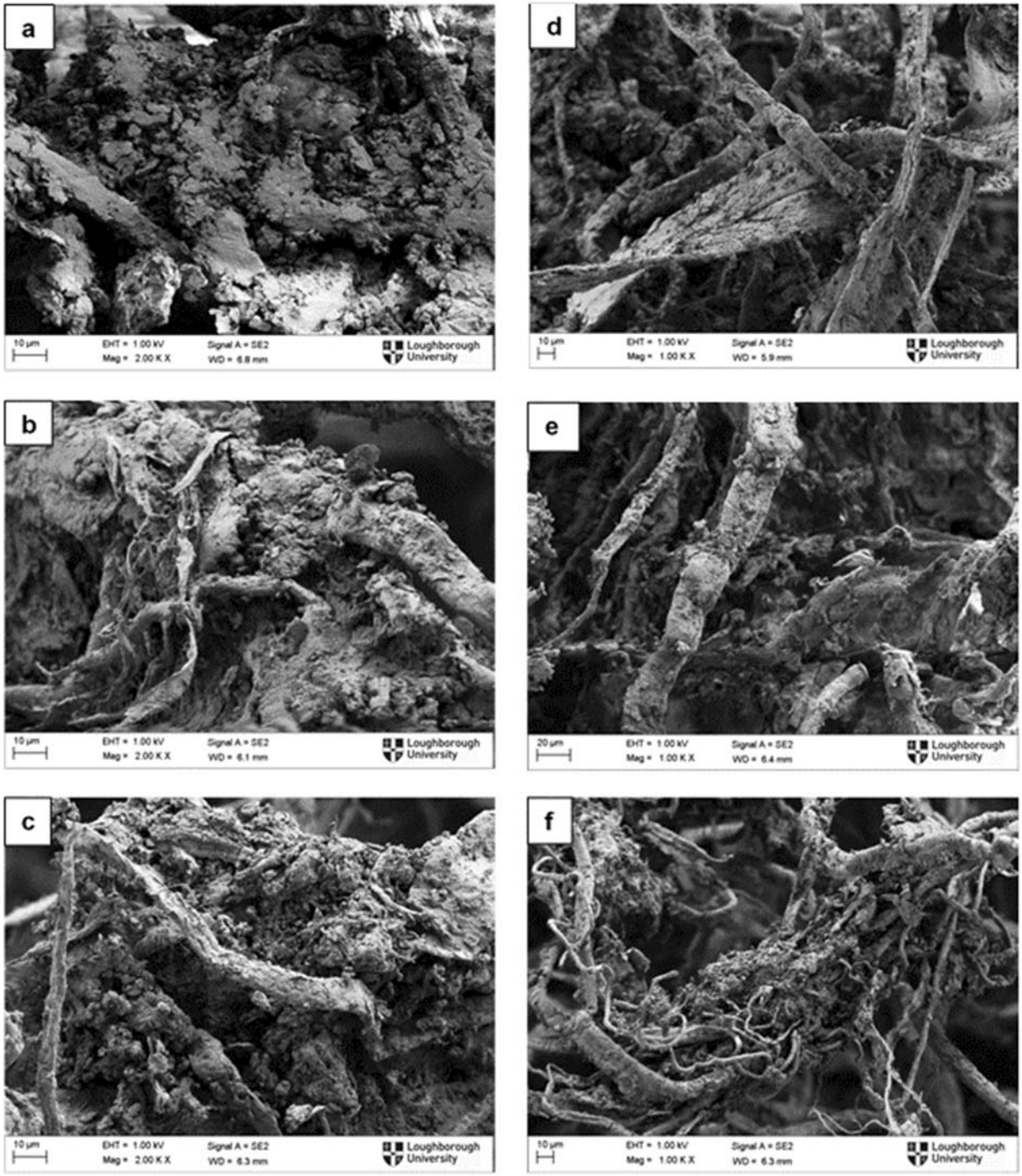

Fig. 1 SEM images of CAMBI sludge hydrochars: (**a**, **d**) no activation; (**b**, **e**) KOH-activated and (**c**, **f**) KOH + HCl-activated

non-activated and activated FS and CAMBI hydrochars. All the hydrochars were found to have a pore size width in the range of mesopores ($1.5 \div 1.6 < r < 100 \div 200$ nm). This mesopore classification follows the Thomson-Kelvin capillary condensation equation, which allows monomolecular, polymolecular and finally, pore-filling through capillary condensation (Zdravkov et al. 2007).

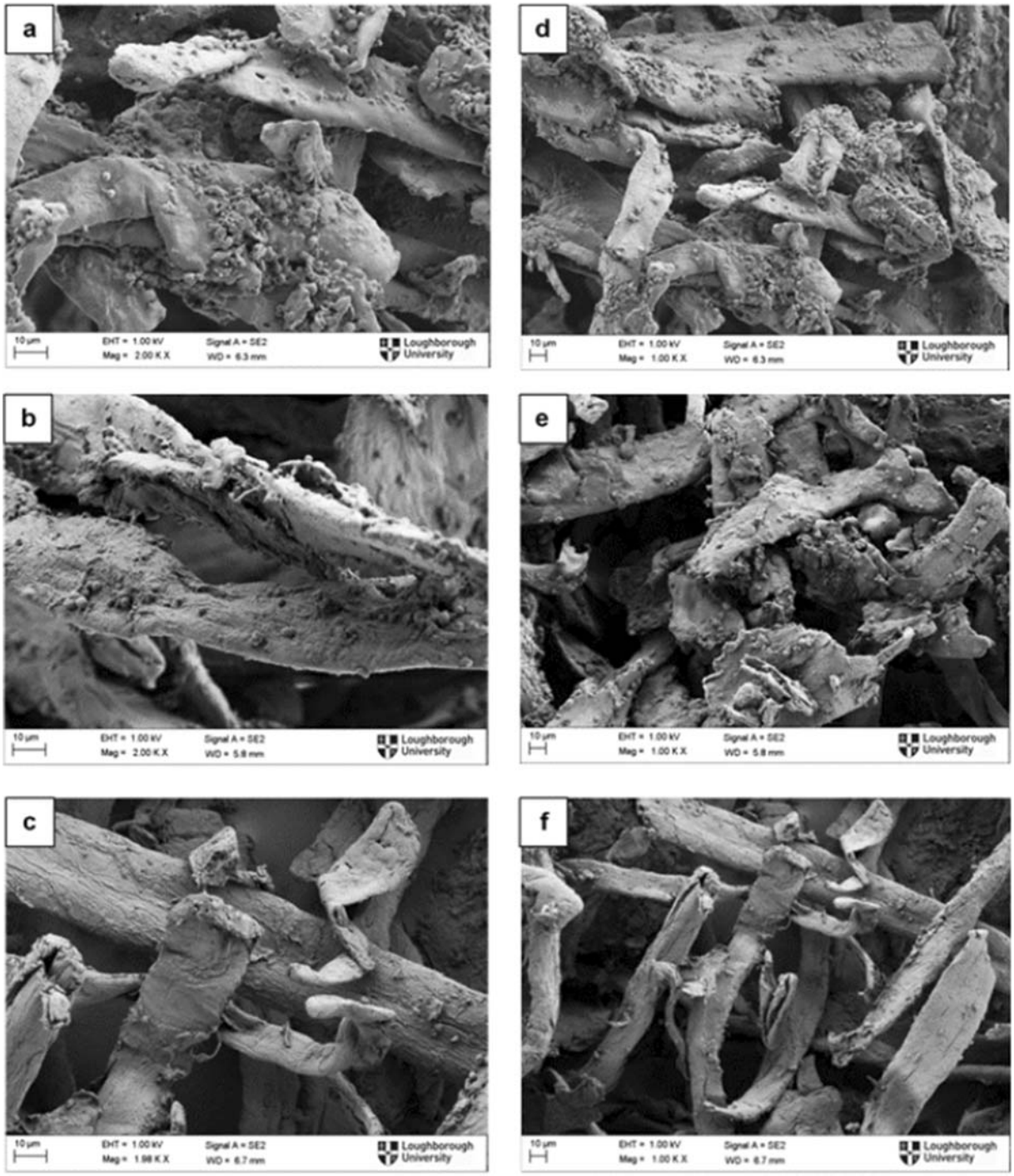

Fig. 2 SEM images of FS hydrochars: (**a**, **d**) no activation; (**b**, **e**) KOH-activated and (**c**, **f**) KOH + HCl-activated

The chemical activations improved the surface area of the hydrochars with CAMBI being most enhanced. KOH activation increased the surface area of CAMBI hydrochar by 2.8 times compared with that of the FS, which did not have any significant increase. The extra HCl activation increased the surface area of the CAMBI hydrochar by 3.2 times, whilst that of the FS hydrochar increased by 2.5 times. Hence, it can be concluded that alkaline and acidic activations physically alter the morphological properties (as indicated by the SEM results)

Table 1 Surface and pore size characteristic of CAMBI and FS-activated and non-activated hydrochars

Hydrochar samples	BET surface area (m^2/g)	Total pore volume (cm^3/g)	BJH adsorption average pore size width (4 V/A) (nm)	BJH desorption average pore size width (4 V/A) (nm)
CAMBI non-activated	0.95	0.047	10.85	20.85
CAMBI + KOH	2.75	0.013	12.09	9.67
CAMBI + KOH + HCl	8.72	0.037	11.69	10.75
FS non-activated	0.41	0.001	10.01	13.57
FS + KOH	0.46	0.001	7.83	11.41
FS + KOH + HCl	1.17	0.003	8.84	11.29

and the pore characteristics of sewage/faecal sludge hydrochars.

The surface area of the benchmark PAC (993 m^2/g) is significantly higher than the range of values obtained for the hydrochars even after chemical activation. Chung et al. (2017) reported higher surface area of 25.3 m^2/g for hydrochar of sewage sludge, which in contrast to the results in this study was decreased to 18.5 m^2/g following KOH activation.

3.3 Surface Functional Groups

FTIR spectra of CAMBI (Fig. 11 in the Appendix) show similar peaks for the non-activated hydrochar and the activated (KOH and KOH + HCl) hydrochars. This indicates that the chemical activation did not appreciably alter the composition of the surface functional groups of the hydrochars. The broad bands between 3200 and 3400 cm^{-1} could be due to OH stretching vibrations in the hydroxyl and carboxyl groups. The features at around 2916 and 2849 cm^{-1} are attributed to aliphatic C–H stretching vibrations. Two bands at 1600 and 1500 cm^{-1} can be due to C=C rings (stretching vibrations), and consequently, those at 1330–1430 cm^{-1} could be attributed to O–H bending. The bands between 1800 and 2300 cm^{-1} showing in the non-activated and KOH-activated hydrochars may be noise signals.

After activation, a less intense vibration of C–H was detected at the bands between 2850 and 2920 cm^{-1}. This could be due to OH deprotonation of the CAMBI hydrochar surface, which moreover remained after the further treatment with HCl. To summarise, the CAMBI hydrochars contain carboxyl acids groups and derivatives.

The spectra for the FS hydrochars (Fig. 12 in the Appendix) is similar to the CAMBI ones, because the materials are comparable. Similarly, wide bands at 3200–3400 cm^{-1} and sharp features at 2851–2969 cm^{-1}, respectively correspond to OH stretching and C–H stretching vibrations. After activation, the OH stretch band was more intense than the C–H and C=O bands, which was strongly observed after the FS + KOH hydrochar was further treated with HCl. The remaining bands at 1650–1550 cm^{-1} and at 1400 cm^{-1} could be attributed to C=O and C=C bonds.

3.4 Adsorption Efficiency

Effluent of the anaerobic digestion of HTC wastewater contained TOC levels of 3.4 g/L and COD of 15.0 g/L. FS hydrochar (non-activated) was used to conduct the initial set of tests. This resulted in a COD removal of 18.0–33.0% and that of TOC of 41.0–44.0% for a contact time of 4–6 h. However, the results were not satisfactory as the effluent still contained high levels of COD between 10.1 and 12.3 g/L and TOC of about 2.0 g/L. The maximum compliance limit of COD allowed in wastewater before discharge is 0.25 g/L O_2 (UKEA 2019). Also, there were high fluctuations in the results, and the reproducibility was poor.

Activation of hydrochars has been found to improve adsorption capacity. KOH has been reported as an effective activation additive (Spataru et al. 2016; Koottatep et al. 2017). HCl has also been found as an additional additive, after addition of KOH (Hameed et al. 2007; Qiu et al. 2009; Sevilla and Fuertes 2011) or during the HTC process, to improve the adsorption efficiency of hydrochars. However, these studies have objectives different from those of the present study, although their findings on KOH and HCl activations

are useful for comparison with that of this work. Hence, in the next experiments, the hydrochars were activated to obtain KOH hydrochars and KOH + HCl hydrochars of CAMBI and FS.

3.4.1 Effect of Activation on Adsorption Efficiency

Figure 3 shows TOC removal after activation of the CAMBI and FS hydrochars. The chemical modification improved the adsorption efficiency of the hydrochars, increasing the percentage of COD and TOC removed. Adsorption was stable for the KOH- and HCl-activated hydrochars as compared with the unstable results observed for the non-activated hydrochars. COD removed increased to 60.0% for the FS + KOH hydrochar and 75.0% for the CAMBI + KOH hydrochar compared with 18.0–33.0% for the unmodified hydrochars. As explained in section 3.2 Specific Surface and Pore Size Distribution, chemical activation enhanced the surface characteristics of the hydrochars shown in the BET surface areas and pore size results in Table 1, but it did not alter the composition of the surface functional groups (section 3.3 Surface Functional Groups). Hence, it can be said that the improvement of adsorption efficiency after KOH activation was due to the increase in the surface area and pore size of the hydrochars that provided adequate adsorptive sites and internal pore structure for adsorption, but not caused by the change in composition of the surface functional groups.

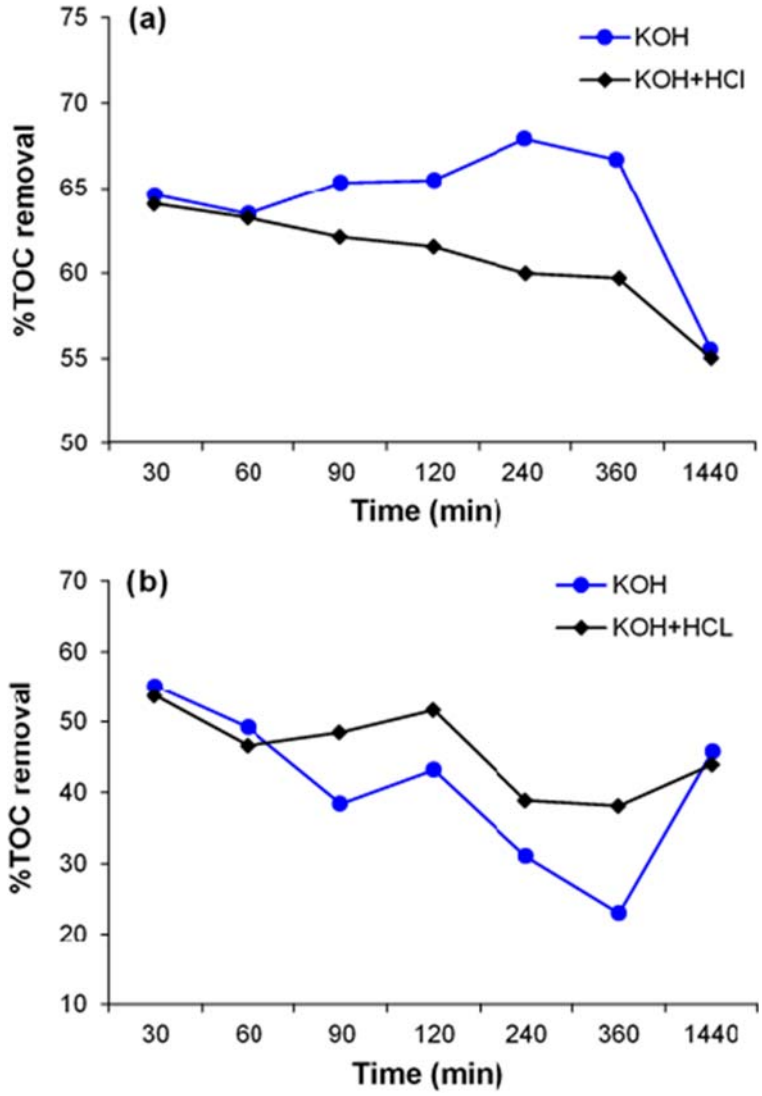

Fig. 3 Percentage of TOC removal for activated hydrochars at natural pH of the effluent: (**a**) CAMBI hydrochars and (**b**) FS hydrochars

However, for the FS + KOH hydrochar, the increase in surface area was not significant, which may explain the less improvement in the adsorption of COD and TOC compared with that of CAMBI + KOH, although the amelioration is remarkably higher than that of the unmodified FS hydrochar. A possible reason could be due to the change in the hydrophobicity of the FS hydrochar surface as the KOH treatment may have activated more hydrophobic sites. This is because hydrochar is generally characterised by a hydrophobic interior, which is stabled banded with the hydrophilic external surface (Sevilla and Fuertes 2009; Roldán et al. 2012), and the main component of wastewater is found to be hydrophobic (Khan et al. 2013). Chung et al. (2017) reported an increase in *Escherichia coli* removal even though there was a decrease in the surface area of the sewage sludge hydrochar activated with KOH.

The additional HCl activation did not significantly improve the efficiency of the adsorption capacity of the CAMBI hydrochar, remaining almost alike, about 64.0% and 76.0% for the highest TOC and COD adsorbed, respectively. This is inconsistent with the BET results, as surface area of the CAMBI + KOH + HCl hydrochar was found to be 3 times higher than that of the CAMBI + KOH hydrochar. However, the further HCl activation enhanced the adsorption capacity of the FS + KOH hydrochar and stabilised its performance, with 79.0% of the initial COD adsorbed, an increase of 21.0%. This result is supported by the surface area results, as the surface area of the FS + KOH hydrochar was increased by 2.5 times after the extra HCl treatment.

It must be noted that these experiments were conducted by maintaining the natural pH conditions, which were between 7.8 and 8.0.

3.4.2 Effect of pH on Adsorption Efficiency

One of the important parameters that could influence adsorption is pH. Hence, the effect of pH on removal of TOC (i.e. the ratio of remaining to initial TOC concentration) was investigated. As shown in Fig. 4, the adsorption capacity of the activated hydrochars of CAMBI and FS decreased significantly as the pH increased from 2 to 9. This means that an anion sorption may be taking place, and the surface of the hydrochars is cationic type, which is predominant with H^+. At higher pH, the OH^- ions present compete with the organics for binding sites on the hydrochar surface, resulting in lower sorption capacity. At lower pH, however, the H^+ ions in the wastewater did not interfere with the sorption of the organics, which increased their removal, most likely by ion exchange sorption.

The PAC resulted in the highest removal efficiency of organics, which was equivalent to 88.0–278.0 mg/L of the TOC measured in the effluent. As shown in Fig. 4e, the change in pH did not significantly affect the adsorption capacity of the PAC.

3.4.3 Effect of Contact Time on Adsorption Efficiency

The results presented in Fig. 5 and Table 2 indicate that contact time and additional HCl activation of FS + KOH and CAMBI + KOH hydrochars did not have significant effect on the removal of organic pollutants from the AD effluent. To investigate the probability of a fast COD removal due to chemical precipitation, an experiment was performed without using any hydrochar with and without the addition of HCl at a low pH. However, there was no COD removal. This might be because the reaction was rapid and occurred before the 30 min, so it was not possible to record in this work. Chung et al. (2017) made a similar observation when using sewage sludge–derived hydrochar activated with KOH for the removal of *Escherichia coli*. A further investigation would be required to explain these reactions; however, this is beyond the scope of this work.

3.4.4 Effect of Adsorbent Dose on Adsorption Efficiency

In order to investigate the influence of adsorbent dose on removal of organics from the AD effluent, adsorption was carried out using adsorbent doses between 1.0 and 70.0 g/L for a contact time of up to 1440 min. PAC and KOH + HCl hydrochars were used as the combined activations have resulted in increased COD/TOC removal. As shown in Fig. 6, for PAC, COD removal increased steadily with increasing adsorbent dose up to 30.0 g/L and remained constant afterwards. However, increasing the dose of CAMBI and FS hydrochars did not affect COD removal as it remained nearly constant between 10 and 70 g/L. The possible reason is not known, although it could be an interference during the adsorption process or the suitable range of doses were not used. Hence, a further study may be needed to understand this trend.

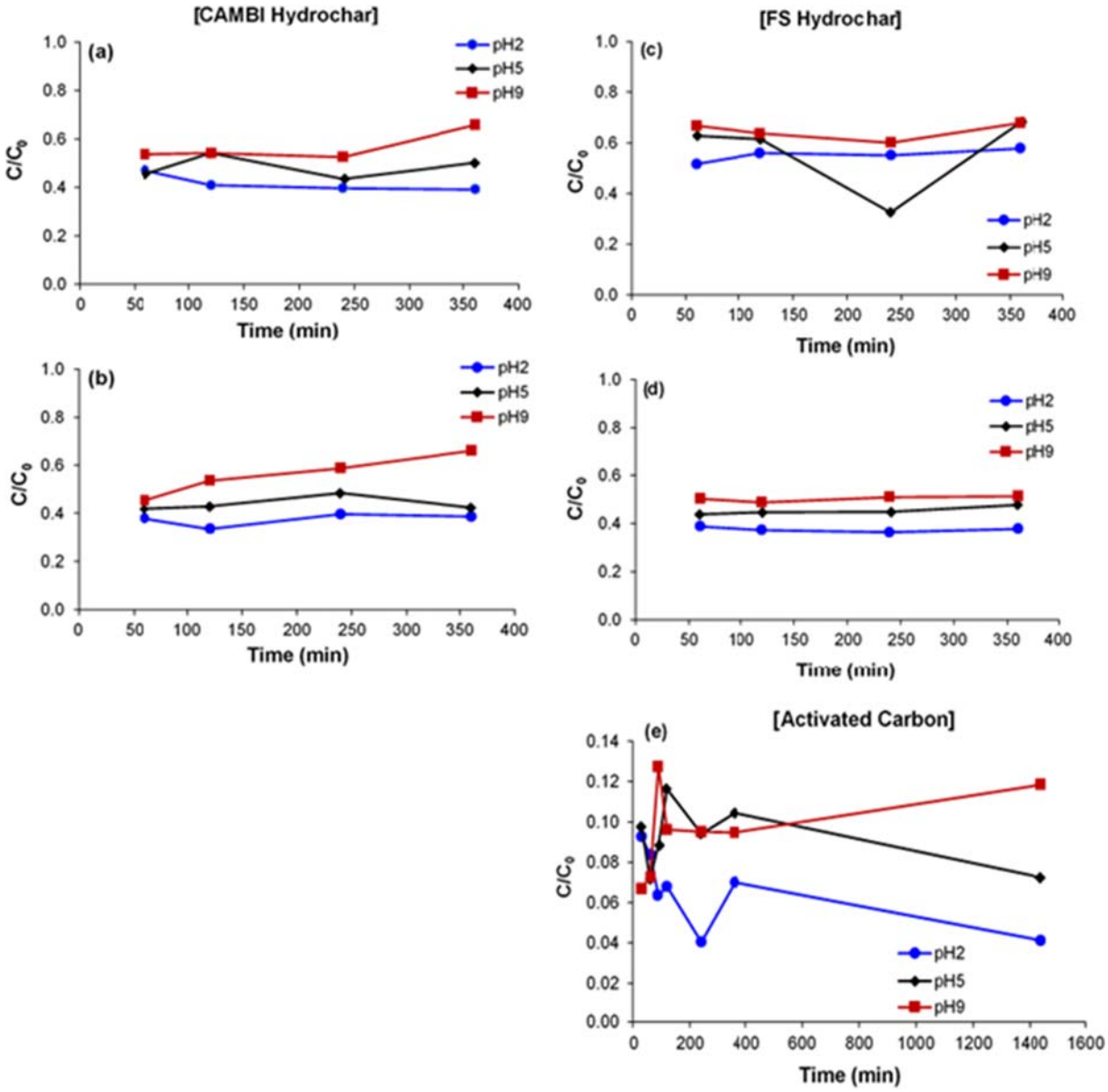

Fig. 4 Effect of pH on TOC adsorption capacity using activated CAMBI and FS hydrochars and activated carbon: (**a**) CAMBI + KOH; (**b**) CAMBI + KOH + HCl; (**c**) FS + KOH; (**d**) FS + KOH + HCl and (**e**) powdered activated carbon (PAC)

3.5 Adsorption Kinetics

In this work, the pseudo-first- and -second-orders, intraparticle diffusion and Elovich kinetic models (shown in Figs. 7 and 8) were used to study the adsorption of organic pollutants in AD effluent. Of all the kinetic models used in this study, the experimental data satisfactorily fit onto the pseudo-second-order kinetic model compared with the other models. The high R^2 values obtained are shown in Fig. 7d–f and Table 3, and the kinetic constants calculated for each adsorbent at pH 5 presented in Table 3. The results indicate that the adsorption took place by chemisorption mechanism rather than physisorption. This means that a chemical bond was the attracting force between the adsorbents and the adsorbate, and that the molecules accumulated and formed a monolayer.

The range of values report for the kinetic constant, k, differs. For example, Verma et al. (2014) using GAC obtained a k value of $8.9 \times 10^{-0.4}$ g/mg min for COD adsorption, whilst Aluyor and Badmus (2008) reported

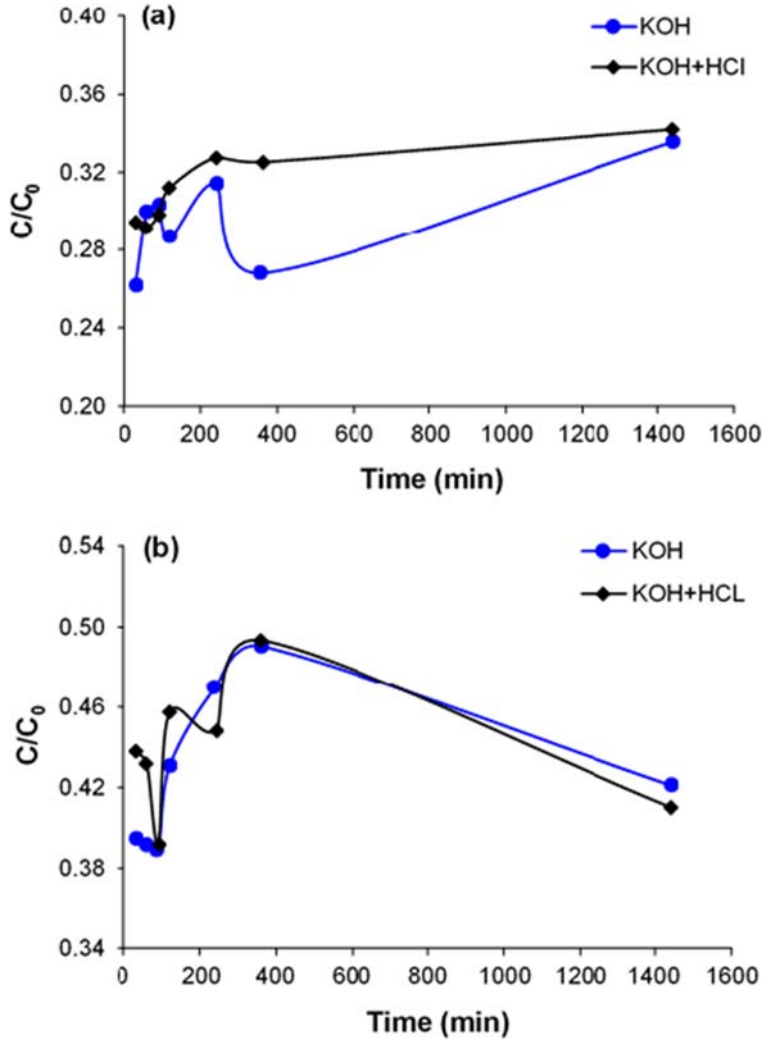

Fig. 5 Effect of contact time on TOC removal for activated hydrochars at pH 5: (**a**) CAMBI hydrochar and (**b**) FS hydrochar

k values of 3.52 and 0.0499 g/mg min, and Koottatep et al. (2017) had a *k* value of 0.0034 g/mg min for the adsorption of Cu. The constants obtained from this study are within the range of values reported by Koottatep et al. (2017), but the absorbates are different so no clear comparison can be made with their studies.

Table 2 TOC and COD removal efficiency by activated CAMBI and FS hydrochars at pH 5

Adsorbents	% Removal	
	TOC	COD
CAMBI + KOH	73.8 (± 2.59)	79.5 (± 2.77)
CAMBI + KOH + HCl	70.6 (± 1.92)	78.6 (± 2.32)
FS + KOH	57.9 (± 4.01)	70.2 (± 3.56)
FS + KOH + HCl	56.2 (± 3.28)	77.6 (± 2.86)
PAC (neutral pH)	98.6 (± 1.19)	90.8 (± 2.19)

The CAMBI hydrochars have higher values of the amount adsorbed at equilibrium (q_e) compared with that of FS and PAC. For both CAMBI and FS, the q_e values were higher after the extra HCl treatment, which means that the additional HCl activation of FS and CAMBI hydrochars increased the amounts of organics adsorbed at equilibrium. The extremely lower q_e value of the FS + KOH hydrochar means that a higher dose of this adsorbent would be needed in order to achieve efficient adsorption. However, Aluyor and Badmus (2008), in their work using activated carbon from horn in a dose of 90 g/L, obtained a low q_e of 0.7224 mg/g but achieved a high COD removal of about 95.0%, which

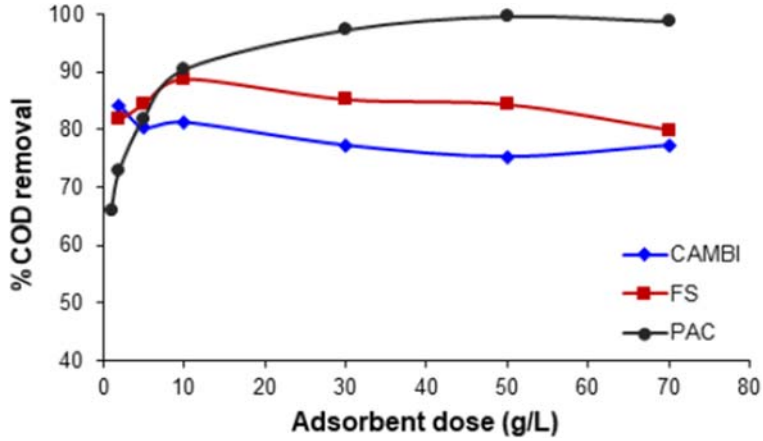

Fig. 6 Effect of adsorbent dose on the percentage of COD removed for CAMBI and FS hydrochars activated with KOH and HCl, and PAC for adsorption at pH 5 and a contact time of 1440 min

may be due to the generally high BET surface area of activated carbons.

Intraparticle diffusion model may also describe the adsorption of the organic contaminants onto CAMBI hydrochar activated with KOH (i.e. CAMBI + KOH) as a reasonably high R^2 value of 0.972 was obtained (Fig. 8b). However, the linear plot did not pass through the origin, which is an indication of some degree of boundary layer control (Arami et al. 2008), and this further means that intraparticle diffusion was not the only rate-controller step, but rather, pseudo-second-order kinetic model controlled the rate of adsorption, and all of which may have operated simultaneously.

The Elovich equation, which also describes second-order kinetics or chemisorption process, may also describe the adsorption of the organic contaminants onto the CAMBI hydrochars activated with KOH and HCl (Fig. 8e and Table 3). This model assumes that the actual adsorbent surfaces are energetically heterogeneous. However, the initial adsorption rates (α) were too large to calculate, and the desorption constants (β) have negative values, which indicate that the Elovich equation cannot be used to propose the adsorption kinetics of the CAMBI activated hydrochars.

3.6 Adsorption Isotherms

The adsorption isotherms describe how the adsorbates interact with the adsorbents. In order to investigate the adsorption capacity of organic pollutants in the AD effluent onto FS and CAMBI hydrochars and PAC, the experimental data were fitted to the three most common isotherm models for describing solid-liquid adsorption processes as shown in Fig. 9. In general, it was difficult to obtain a better fit to the adsorption isotherms, which may be due to the complex nature of AD effluent used in this study, which contained several organics. According to Tan et al. (2015), the adsorption mechanism of a complex wastewater may combine with other types of interactions such as electrostatic attraction, hydrogen bonding, pore-filling and hydrophobic interactions.

Initially, the COD data were used, but that did not yield meaningful plots. Also, an attempt was made to use the Redlich-Peterson isotherm model, which is a hybrid and combines elements from both the Langmuir and Freundlich equations, but all plots had negative slopes. Hence, this isotherm model was not considered in this study.

The isotherm parameters presented in Table 4 indicate that except for FS + KOH hydrochar and comparatively PAC, the Freundlich and Langmuir isotherm models produced high correlation coefficient, R^2 values (> 0.9). Also, the Freundlich isotherm model gave a high R^2 value (> 0.9) for adsorption using FS + KOH + HCl hydrochar. However, for a satisfactory adsorption, the Freundlich constant n (which represents the energetic heterogeneity of the adsorption sites) should take values in the range 1.0–10.0. Hence, adsorption of organic pollutants in the AD effluent onto FS and CAMBI hydrochars and PAC does not match well with the Freundlich isotherm model. For PAC, the n value is 1.29 and $K_F = 5.00$ mg TOC adsorbed/g PAC, which is lower than values reported by Aluyor and Badmus (2008) for COD adsorption with a similar material; K_{CAC} of 13.71 for commercial activated carbon (CAC) and K_{AHC} of 9.86 mg/g for activated carbon from animal horn (ACH).

The Langmuir isotherm model (Fig. 9c) produced negative intercept values for adsorption using CAMBI +

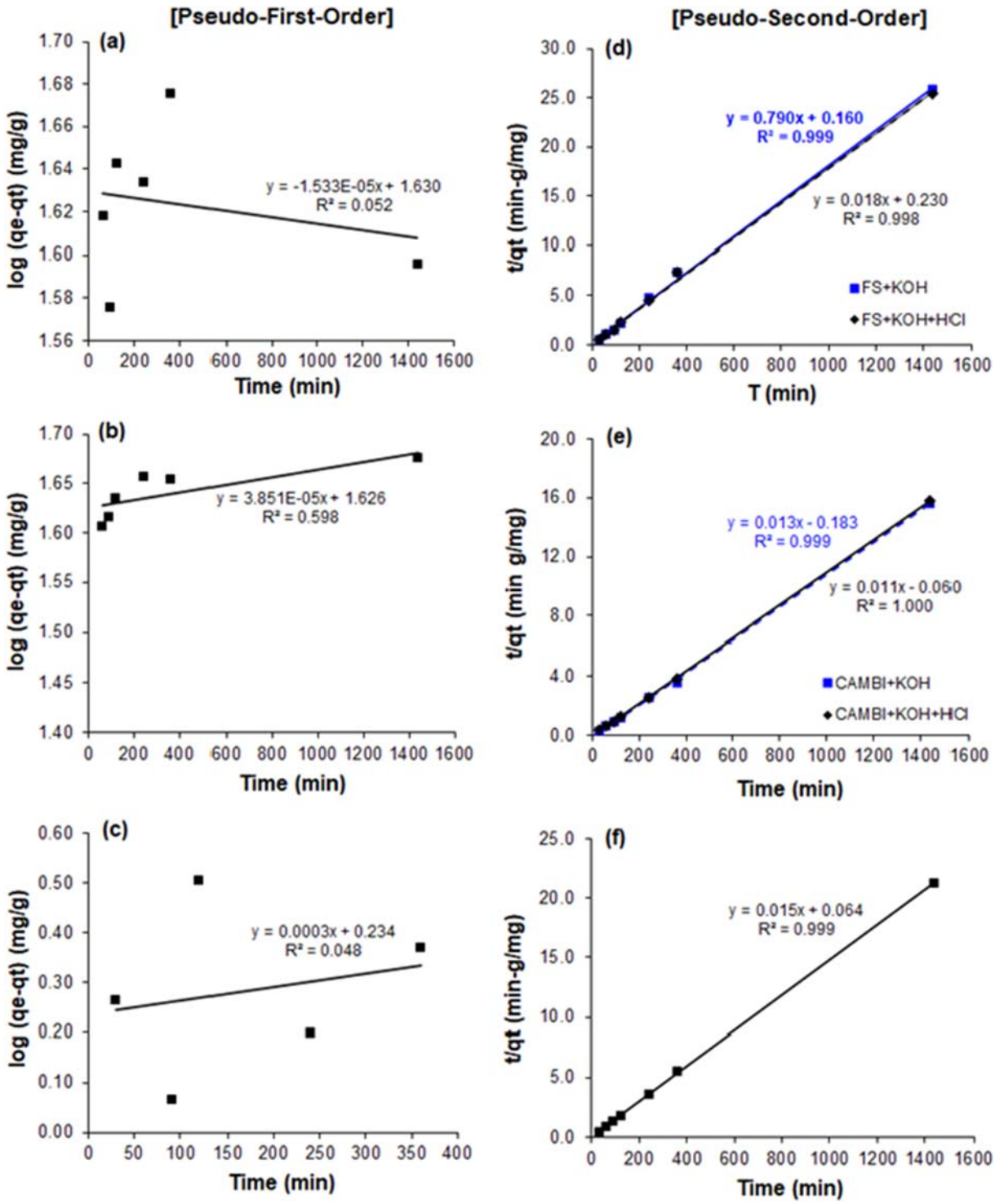

Fig. 7 Pseudo-first-order (**a**–**c**) and pseudo-second-order (**d**–**e**) adsorption kinetic models using hydrochars and activated carbon for TOC adsorption at pH 5: (**a**) FS + KOH + HCl , pseudo-first-order; (**b**) CAMBI + KOH + HCl, pseudo-first-order; (**c**) PAC, pseudo-first-order; and (**f**) PAC, pseudo-second-order. The variables *x* and *y* in the linear regression equations have been defined in Table 3

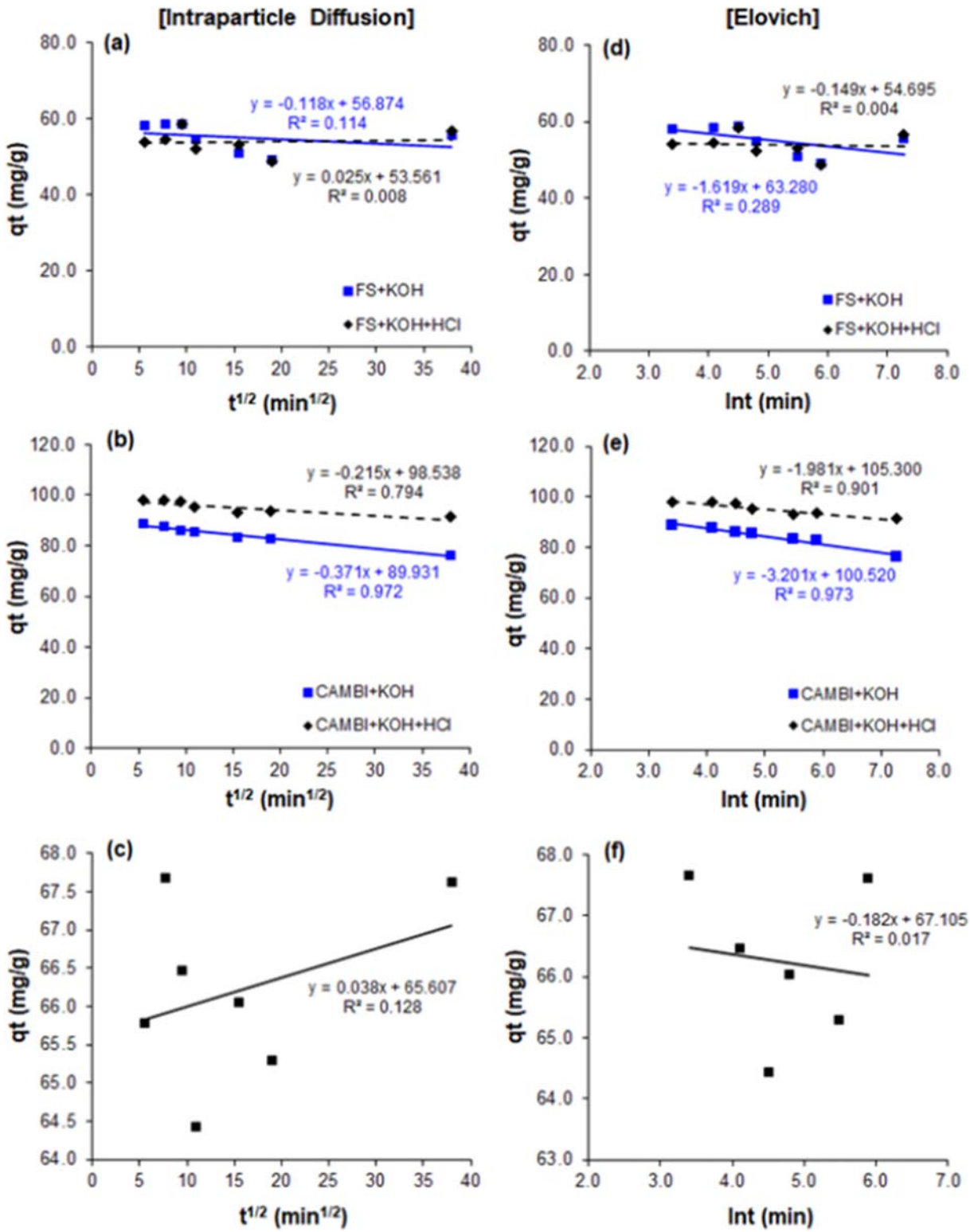

Fig. 8 Intraparticle diffusion (**a**–**c**) and Elovich (**d**–**e**) adsorption kinetic models using hydrochars and activated carbon for TOC adsorption at pH 5: (**c**) PAC, intraparticle diffusion model and (**f**) PAC, Elovich model. The variables *x* and *y* in the linear regression equations have been defined in Table 3

Table 3 Comparison of kinetic parameters of the investigating TOC adsorbents at pH 5

Kinetic model	Parameter	Adsorbents (hydrochars)				
		FS + KOH	CAMBI + KOH	FS + KOH + HCl	CAMB + KOH + HCl	PAC
Pseudo-first-order	k_1 (min^{-1})	–	–	2.0×10^{-5}	-4.0×10^{-5}	3.0×10^{-4}
	R^2	–	–	0.052	0.598	0.048
Linear regression	$y = \ln(q_e - q_t)\ x = k_1$			$y = -1.53 \times 10^{-5}x + 1.63$	$y = -3.8510^{-5}x + 1.63$	$y = 0.0003x + 0.234$
Pseudo-second-order	k_2 (g/mg min)	3.90	9.53×10^{-4}	1.35×10^{-3}	2.03×10^{-3}	3.43×10^{-3}
	R^2	0.999	1.000	0.998	1.000	1.000
	q_e (mg/g)	1.27	75.76	56.82	90.91	67.57
Linear regression:	$y = t/q_t\ x = 1/q_e$	$y = 0.790x + 0.160$	$y = 0.013x - 0.183$	$y = 0.018x + 0.230$	$y = 0.011x + 0.060$	$y = 0.015x + 0.064$
Intraparticle diffusion	k_3 (mg/g $min^{1/2}$)	−0.12	−0.37	0.03	−0.22	0.04
	C	56.87	87.93	53.56	98.54	65.61
	R^2	0.114	0.972	0.008	0.794	0.127
Linear regression	$y = q_t\ x = k_3$	$y = 0.118x + 56.874$	$y = -0.215x + 98.538$	$y = 0.025x + 53.561$	$y = -0.371x + 89.931$	$y = 0.038x + 65.607$
Elovich	α (mg/g min)	4.70×10^{54}	Indefinite	5.00×10^{54}	Indefinite	1.39×10^{29}
	β (g/mg)	−0.62	−0.31	−6.72	−0.51	−5.50
	R^2	0.289	0.973	0.004	0.901	0.017
Linear regression	$y = q_t\ x = 1/\beta$	$y = -1.619x + 63.280$	$y = -3.201x + 100.520$	$y = -0.149x + 54.695$	$y = -1.981x + 105.300$	$y = -0.182x + 67.105$

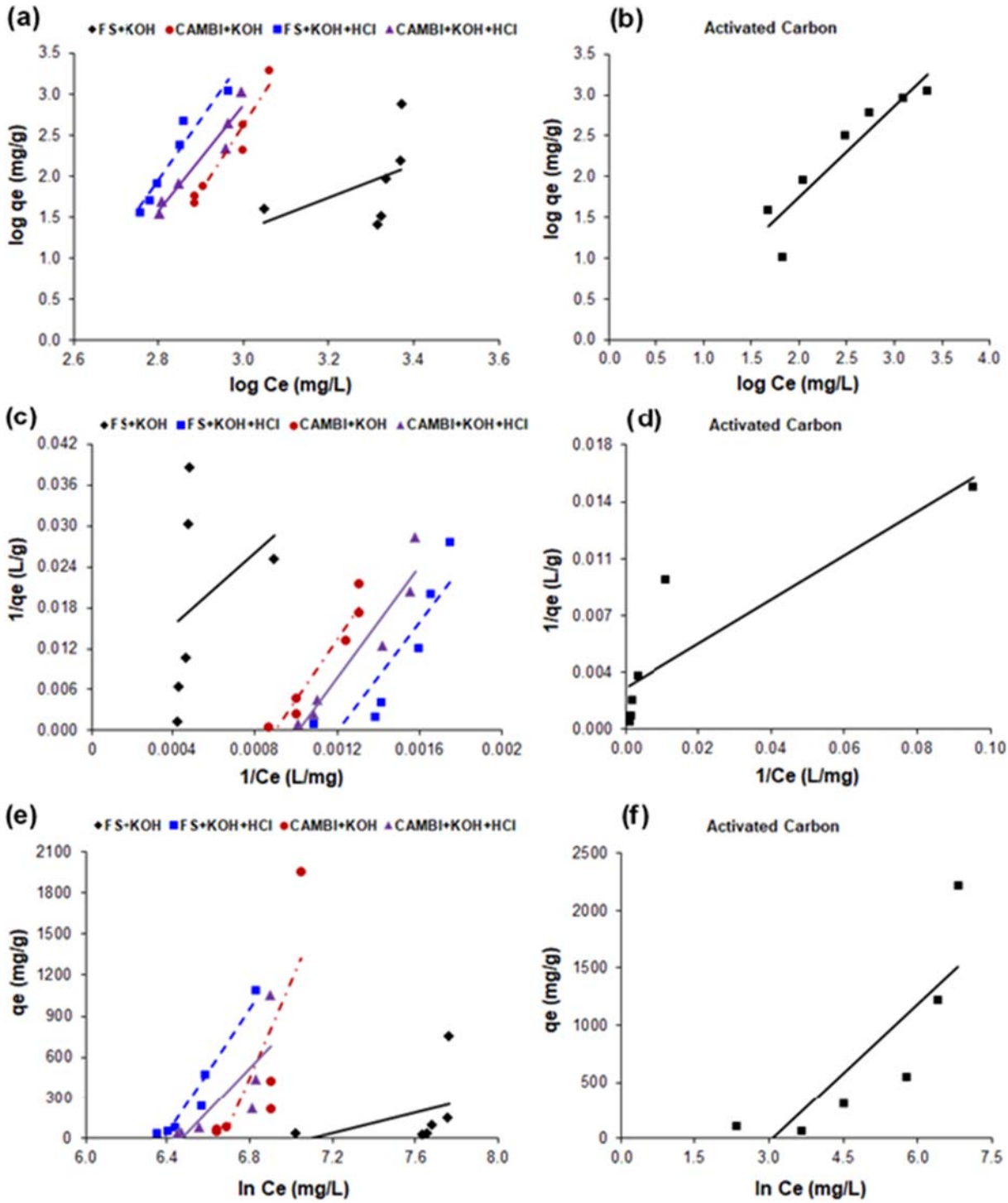

Fig. 9 Adsorption isotherms of TOC adsorption at pH 5: (**a**) Freundlich model for FS and CAMBI hydrochars; (**b**) Freundlich model for PAC; (**c**) Langmuir model for FS and CAMBI hydrochars; (**d**) Langmuir model for PAC; (**e**) Temkin model for FS and CAMBI hydrochars and (**f**) Temkin model for PAC

KOH, FS + KOH + HCl and CAMBI + KOH + HCl, which in addition to negative parameters shown in Table 4 indicate that the data do not match with Langmuir model. Langmuir model for adsorption using FS + KOH resulted

Table 4 Analysis of adsorption of organic pollutants on faecal sludge and CAMBI hydrochars based on different adsorption isotherm models

Isotherm model	Parameter	Adsorbents (hydrochars)				
		FS + KOH	CAMBI + KOH	FS + KOH + HCl	CAMBI + KOH + HCl	PAC
Freundlich	n	0.492	0.123	0.134	0.155	1.29
	K_F (mg/g)	1.73×10^{-5}	1.64×10^{-22}	9.68×10^{-20}	3.03×10^{-17}	5.00
	R^2	0.204	0.940	0.926	0.939	0.864
Langmuir	b (L/mg)	1.67×10^{-4}	-8.99×10^{-4}	-1.20×10^{-3}	-1.01×10^{-3}	0.02
	q_m (mg/g)	222.22	−25.13	−20.79	−23.87	400.00
	R_L	0.66	−0.26	−0.21	−0.24	0.02
	R^2	0.109	0.929	0.784	0.917	0.785
Temkin	b_T	6.51	0.70	1.08	1.55	6.14
	A_T (g/mg)	8.24×10^{-4}	1.26×10^{-3}	1.69×10^{-3}	1.55×10^{-3}	0.05
	R^2	0.143	0.654	0.939	0.653	0.693

in a very low R^2 value, but the efficiency of adsorption (R_L) value (0.66) is less than 1. This means adsorption of organic pollutants onto FS + KOH may be favourable according to the Langmuir isotherm model. The lowest R_L value corresponds to the commercial PAC with relatively higher R^2 value and higher adsorption capacity (q_m), which indicates a favourable behaviour towards TOC adsorption. Generally, a good sorbent requires low values of b and high values of q_m (Kim et al. 2018).

The efficiency of the adsorption process was predicted by the dimensionless equilibrium parameter, R_L, which is defined by the following equation:

$$R_L = \frac{1}{1 + b.C_0} \tag{13}$$

where C_0 is the initial TOC level in the AD effluent (mg/L). The adsorption is considered irreversible when $R_L = 0$, favourable when $0 < R_L < 1$, linear when $R_L = 1$, and unfavourable when $R_L > 1$.

As shown in Fig. 9e) and Table 4, Temkin adsorption model favours KS + KOH + Cl hydrochar with a higher R^2 value than that of the Freundlich model. Also, because Langmuir and Freundlich models were not favourable for CAMBI + KOH and CAMBI + KOH + HCl hydrochars, although the R^2 values from Temkin model is relatively moderate (> 0.6), the adsorption process with both hydrochars could be taken to follow the Temkin model. The Temkin model (Temkin and Pyzhev 1940) suggests that because of adsorbate-adsorbate interactions, the heat of adsorption should decrease linearly with the surface coverage. The application of the Temkin model is relevant because the oxygenated surface groups discussed in section 3.3 Surface Functional Groups makes the adsorbate-absorbate interactions relevant in the adsorption of organics onto the hydrochars.

In order to understand the adsorption isotherm better, the data obtained from the BET adsorption analyses were used to plot the isotherm graphs presented in Fig. 10. The plots correlated well with the adsorption isotherm types II and IV of the BET adsorption theory, which do not follow the Langmuir constrains. This indicates that the adsorption was polymolecular in the microporous hydrochars and formed because of the interactions between the hydrochar surface and the adsorbate. This supports the earlier discussion in section 3.2 Specific Surface and Pore Size Distribution that the hydrochars have mesopore pore size, allowing monomolecular, polymolecular and pore-filling through capillary condensation. The intermediate region in the isotherm, particularly evident in Fig. 10a and c corresponds to monolayer formation, which is followed by the formation of multilayers. The BET isotherm parameter, C, must be larger than 1.0 which is confirmed for all the hydrochars, as shown in Table 5.

4 Conclusions

This study showed that hydrochars produced from sewage sludge (CAMBI) and faecal sludge (FS) are potential adsorbents for the removal of organic pollutants from an effluent following anaerobic digestion (AD) of HTC wastewater. For both CAMBI and FS hydrochars,

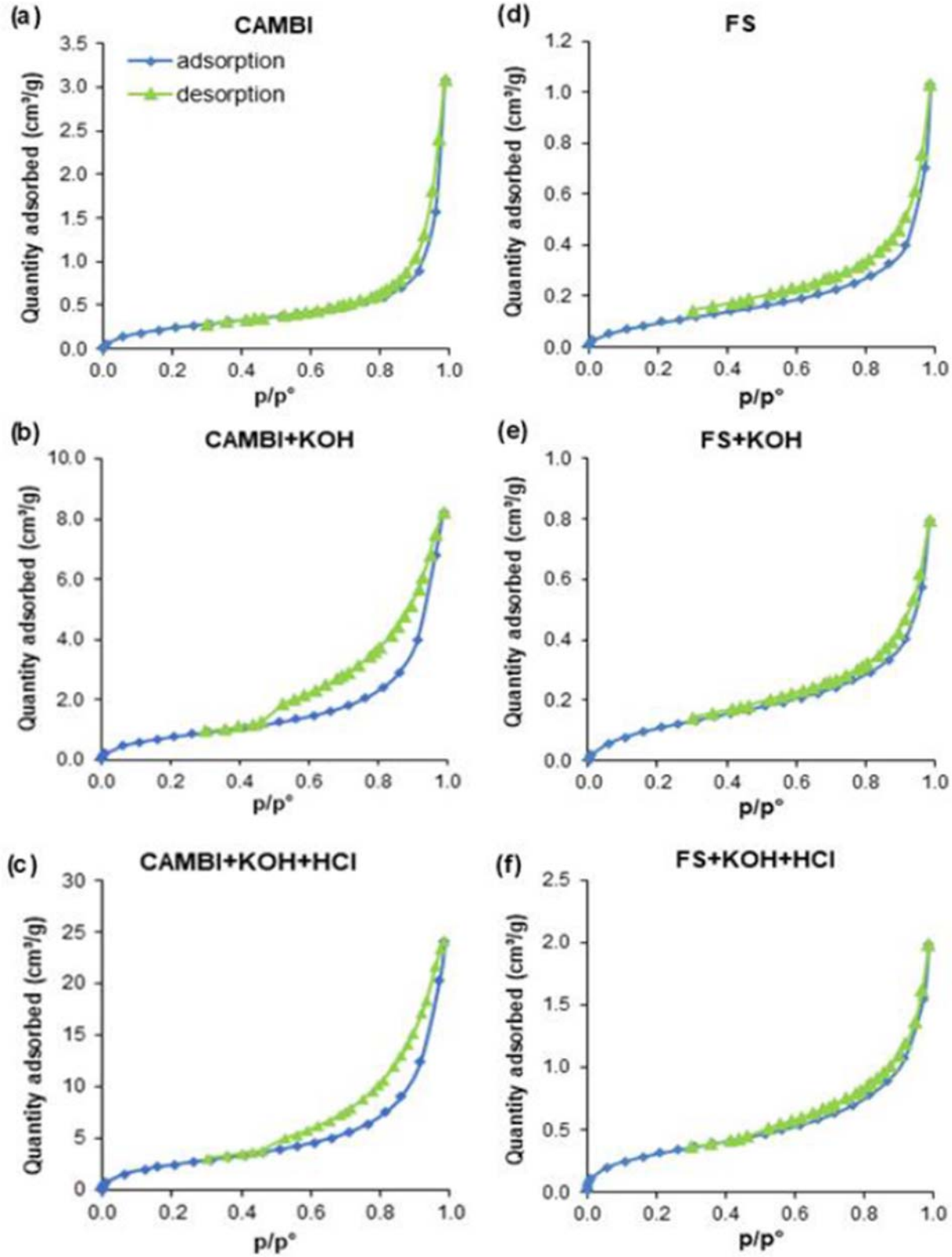

Fig. 10 BET adsorption isotherms for CAMBI and FS hydrochars (activated and non-activated)

Table 5 BET isotherm parameter *C* for the CAMBI and FS hydrochars

Parameter	Adsorbents (hydrochars)					
	CAMBI	CAMBI + KOH	CAMBI + KOH + HCl	SF	SF + KOH	SF + KOH + HCl
C ratio	23.19	27.27	29.35	17.57	16.23	38.83

KOH activation was necessary to stabilise their adsorptivity and improve their efficiency for the removal of organic pollutants from the AD effluent. Extra HCl treatment was needed to improve the adsorption capacity of FS + KOH hydrochar to increase COD removal to 79% compared with 60% after KOH activation, which was contrary to the CAMBI + KOH hydrochar.

Except the benchmark PAC, low pH values increased the adsorption capacity of CAMBI and FS hydrochars activated with KOH and HCl, meaning adsorption of organics was by anion sorption. The kinetics parameters suggested that the adsorption process followed a pseudo-second-order kinetic model. For all adsorbents, the adsorption process correlated well with types II and IV isotherms, proposing a monolayer followed by a multilayer adsorption, with the equilibrium data of CAMBI and FS hydrochars treated with KOH and HCl described by Temkin isotherm model, whilst PAC favoured the Langmuir isotherm model. Therefore, hydrochars derived from sewage sludge and faecal simulant when treated with KOH and HCl are useful adsorbents for removing organic pollutants from anaerobic digester effluent.

Funding Information The authors received the support of the Bill & Melinda Gates Foundation, Seattle, WA, through the Reinvent the Toilet Programme.

Compliance with Ethical Standards

Conflict of Interests The authors declare that they have no conflict of interests.

Appendix

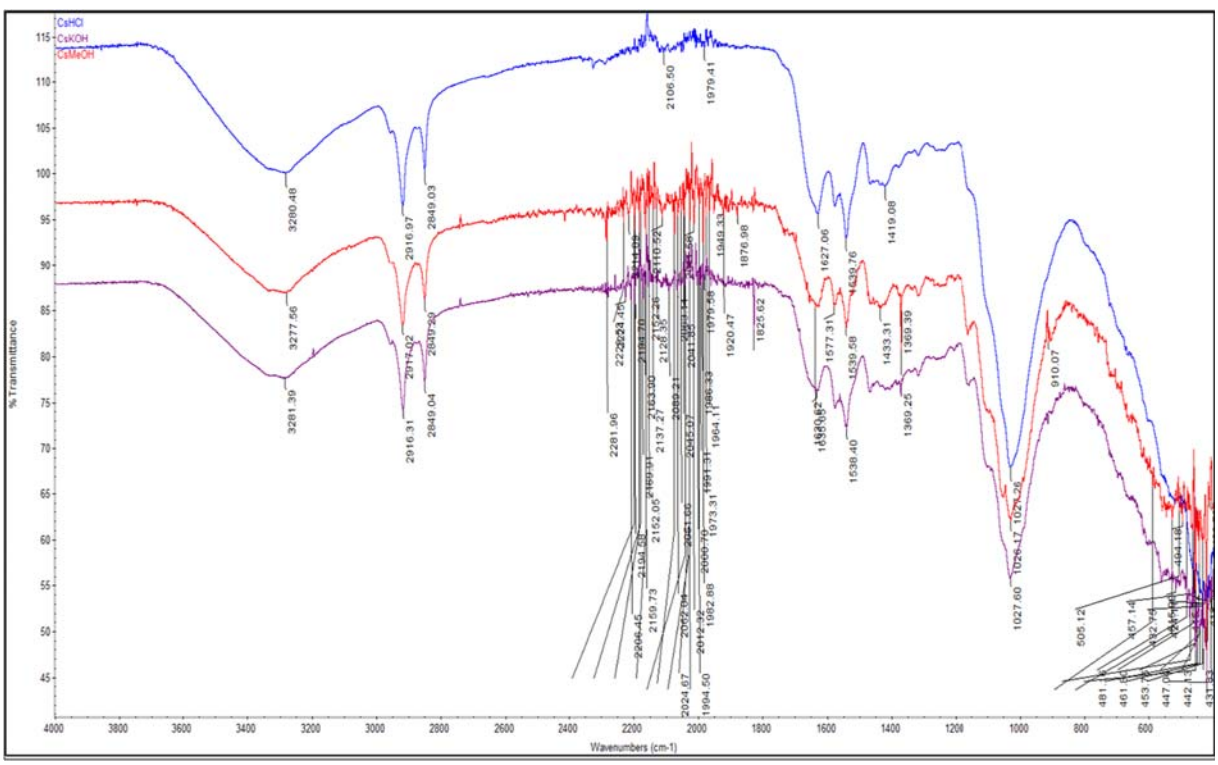

Fig. 11 FTIR spectrum of CAMBI non-activated and activated CAMBI hydrochars

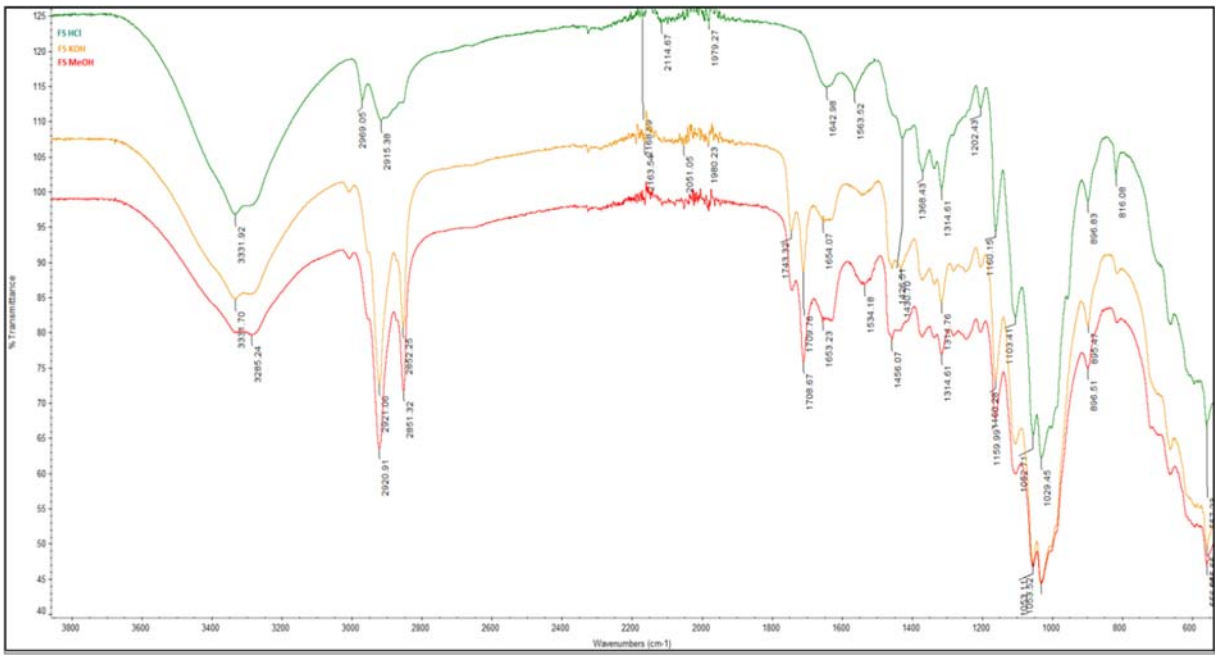

Fig. 12 FTIR spectrum of FS comparing with activated FS hydrochars

References

Ademiluyi, F. T., Amadi, S. A., & Amakama, N. J. (2009). Adsorption and treatment of organic contaminants using activated carbon from waste Nigerian bamboo. *Journal of Applied Sciences and Environmental Management, 13*(3), 39–47.

Alatalo, S. M., Repo, E., Mäkilä, E., Salonen, J., Vakkilainen, E., & Sillanpää, M. (2013). Adsorption behavior of hydrothermally treated municipal sludge and pulp and paper industry sludge. *Bioresource Technology, 147*, 71–76. https://doi.org/10.1016/j.biortech.2013.08.034.

Aluyor, E. O., & Badmus, O. A. M. (2008). COD removal from industrial wastewater using activated carbon prepared from animal horns. *African Journal of Biotechnology, 7*(21), 3887–3891.

Arami, M., Limaee, N. Y., & Mahmoodia, N. M. (2008). Evaluation of the adsorption kinetics and equilibrium for the potential removal of acid dyes using a biosorbent. *Chemical Engineering Journal, 139*, 2–10.

Barrett, E. P., Joyner, L. G., & Halenda, P. P. (1951). The determination of pore volume and area distributions in porous substances. I. Computations from Nitrogen Isotherms. *Journal of the American Chemical Society, 1896*(1948), 373–380.

Cao, X., Ro, K. S., Chappell, M., Li, Y., & Mao, J. (2010). Chemical structures of swine-manure chars produced under different carbonization conditions investigated by advanced solid-state 13C nuclear magnetic resonance (NMR) spectroscopy. *Energy & Fuels, 25*(1), 388–397.

Chen, H., Wan, J., Chen, K., Luo, G., Fan, J., Clark, J., & Zhang, S. (2016). Biogas production from hydrothermal liquefaction wastewater (HTLWW): Focusing on the microbial communities as revealed by high-throughput sequencing of full-length 16S rRNA genes. *Water Research, 106*, 98–107. https://doi.org/10.1016/j.watres.2016.09.05.

Chung, J. W., Foppen, J. W., Gerner, G., Krebs, R., & Lens, P. N. L. (2015). Removal of rotavirus and adenovirus from artificial ground water using hydrochar derived from sewage sludge. *Journal of Applied Microbiology, 119*(3), 876–884.

Chung, J. W., Edewi, O. C., Foppen, J. W., Gerner, G., Krebs, R., & Lens, P. N. L. (2017). Removal of Escherichia coli by intermittent operation of saturated sand columns supplemented with hydrochar derived from sewage sludge. *Applied Sciences, 7*(8), 839. https://doi.org/10.3390/app7080839.

Crini, G. (2006). Non-conventional low-cost adsorbents for dye removal: A review. *Bioresource Technology, 97*(9), 1061–1085.

Danso-Boateng, E., Shama, G., Wheatley, A. D., Martin, S. J., & Holdich, R. G. (2015). Hydrothermal carbonisation of sewage sludge: Effect of process conditions on product characteristics and methane production. *Bioresource Technology, 177*, 318–327. https://doi.org/10.1016/10.1016/j.biortech.2014.11.096.

de La Rubia, M. A., Villamil, J. A., Rodriguez, J. J., Borja, R., & Mohedano, A. F. (2018). Mesophilic anaerobic co-digestion of the organic fraction of municipal solid waste with the liquid fraction from hydrothermal carbonization of sewage sludge. *Waste Management, 76*, 315–322.

Fang, J., Gao, B., Chen, J., & Zimmerman, A. R. (2015). Hydrochars derived from plant biomass under various conditions: Characterization and potential applications and impacts. *Chemical Engineering Journal, 267*, 253–259. https://doi.org/10.1016/j.cej.2015.01.026.

Fernandez, S., Srinivas, K., Schmidt, A. J., Swita, M. S., & Ahring, B. K. (2018). Anaerobic digestion of organic fraction from hydrothermal liquefied algae wastewater by-product. *Bioresource Technology, 247*, 250–258. https://doi.org/10.1016/10.1016/j.biortech.2017.09.030.

Funke, A., & Ziegler, F. (2010). Hydrothermal carbonization of biomass: a summary and discussion of chemical mechanisms for process engineering. *Biofuels, Bioproducts and Biorefining, 4*, 160–177.

Hameed, B. H., & El-Khaiary, M. I. (2008). Kinetics and equilibrium studies of malachite green adsorption on rice straw-derived char. *Journal of Hazardous Materials, 153*, 701–708.

Hameed, B. H., Din, A. T. M., & Ahmad, A. L. (2007). Adsorption of methylene blue onto bamboo based activated carbon: Kinetics and equilibrium studies. *Journal of Hazardous Materials, 141*(3), 819–825.

Ibaraj, S., & Sulochana, N. (2002). Effects of agitation time and adsorbent dosage on the adsorption of dyes. *Indian Journal of Chemical Technology, 9*, 201–208.

Inyang, M., Gao, B., Yao, Y., Xue, Y., Zimmerman, A. R., Pullammanappallil, P., & Cao, X. (2012). Removal of heavy metals from aqueous solution by biochars derived from anaerobically digested biomass. *Bioresource Technology, 110*, 50–56. https://doi.org/10.1016/j.biortech.2012.01.072.

Inyang, M., Gao, B., Zimmerman, A. R., Zhang, M., & Chen, H. (2014). Synthesis, characterization, and dye sorption ability of carbon nanotube-biochar nanocomposites. *Chemical Engineering Journal, 236*, 39–46.

Khan, M. H., Ha, D. H., & Jung, J. (2013). Optimizing the industrial wastewater pretreatment by activated carbon and coagulation: Effects of hydrophobicity/hydrophilicity and molecular weights of dissolved organics. *Journal of Environmental Science and Health, Part A: Toxic/Hazardous Substances and Environmental Engineering, 48*(5), 534–542.

Kim, J., Lee, C., Lee, S. M., Lalhmunsiama, & Jung, J. (2018). Chemical and toxicological assessment of arsenic sorption onto Fe-sericite composite powder and beads. *Ecotoxicology and Environmental Safety, 147*, 80–85. https://doi.org/10.1016/j.ecoenv.2017.08.033.

Klasson, K. T., Ledbetter, C. A., Uchimiya, M., & Lima, I. M. (2013). Activated biochar removes 100% dibromochloropropane from field well water. *Environmental Chemistry Letters, 11*(3), 271–275.

Koottatep, T., Fakkaew, K., Tajai, N., & Polprasert, C. (2017). Isotherm models and kinetics of copper adsorption by using hydrochar produced from hydrothermal carbonization of faecal sludge. *Journal of Water, Sanitation and Hygiene for Development, 7*(*1*), *102–110*. https://doi.org/10.2166/washdev.2017.132.

Lee, C.-G., Hong, S.-H., Hong, S.-G., Choi, J.-W., & Park, S.-J. (2019). Production of biochar from food waste and its applications for phenol removal from aqueous solution. *Water, Air, & Soil Pollution, 230*, 70.

Liu, W.-J., Zeng, F.-X., Jiang, H., & Zhang, X.-S. (2011). Preparation of high adsorption capacity bio-chars from waste biomass. *Bioresource Technology, 102*(17), 8247–8252.

Lu, H., Zhang, W., Yang, Y., Huang, X., Wang, S., & Qiu, R. (2012). Relative distribution of Pb^{2+} sorption mechanisms by sludge-derived biochar. *Water Research, 46*(3), 854–862. https://doi.org/10.1016/j.watres.2011.11.058.

Mohan, D., Sarswat, A., Ok, Y. S., & Pittman Jr., C. U. (2014). Organic and inorganic contaminants removal from water with biochar, a renewable, low cost and sustainable adsorbent – A critical review. *Bioresource Technology, 160*, 191–202.

Mui, E. L. K., Cheung, W. H., Valix, M., & McKay, G. (2010). Dye adsorption onto char from bamboo. *Journal of Hazardous Materials, 177*(1–3), 1001–1005.

Nelson, M., Zhu, L., Thiel, A., Wu, Y., Guan, M., Minty, J., et al. (2013). Microbial utilization of aqueous co-products from hydrothermal liquefaction of microalgae *Nannochloropsis oculate*. *Bioresource Technology, 136*, 522–528. https://doi.org/10.1016/10.1016/j.biortech.2013.03.074.

Nyktari, E., Wheatley, A., Danso-Boateng, E., & Holdich, R. (2017). Anaerobic digestion of liquid products following hydrothermal carbonisation of sewage sludge with different reaction conditions. *Desalination and Water Treatment, 91*, 245–251.

Parshetti, G. K., Hoekman, S. K., & Balasubramanian, R. (2013). Chemical, structural and combustion characteristics of carbonaceous products obtained by hydrothermal carbonization of palm empty fruit bunches. *Bioresource Technology, 135*(3), 683–689.

Qiu, Y., Zheng, Z., Zhou, Z., & Sheng, G. D. (2009). Effectiveness and mechanisms of dye adsorption on a straw-based biochar. *Bioresource Technology, 100*(21), 5348–5351. https://doi.org/10.1016/j.biortech.2009.05.054.

Ramavandi, B., & Farjadfard, S. (2014). Removal of chemical oxygen demand from textile wastewater using a natural coagulant. *Korean Journal of Chemical Engineering, 31*(1), 81–87. https://doi.org/10.1007/s11814-013-0197-2.

Roldán, L., Armenise, S., Santos, I., Fraile, J. M., & García-Bordejé, E. (2012). The formation of a hydrothermal carbon coating on graphite microfiber felts for using as structured acid catalyst. *Carbon, 50*(3), 1363–1372. https://doi.org/10.1016/j.carbon.2011.11.008.

Sevilla, M., & Fuertes, A. B. (2009). Chemical and structural properties of carbonaceous products obtained by hydrothermal carbonization of saccharides. *Chemistry - A European Journal, 15*(16), 4195–4203.

Sevilla, M., & Fuertes, A. B. (2011). Sustainable porous carbons with a superior performance for CO_2 capture. *Energy & Environmental Science, 4*(5), 1765–1771. https://doi.org/10.1039/C0EE00784F.

Spataru, A., Rohan Jain, R., Chung, J. W., Gerner, G., Krebs, R., & Lens, P. N. L. (2016). Enhanced adsorption of orthophosphate and copper onto hydrochar derived from sewage sludge by KOH activation. *RSC Advances, 6*(104), 101827–101834.

Sun, K., Ro, K., Guo, M., Novak, J., Mashayekhi, H., & Xing, B. (2011). Sorption of bisphenol A, 17α-ethinyl estradiol and phenanthrene on thermally and hydrothermally produced biochars. *Bioresource Technology, 102*(10), 5757–5763.

Tan, X., Liu, Y., Zeng, G., Wan, X., Hu, X., Gu, Y., & Yan, Z. (2015). Application of biochar for the removal of pollutants from aqueous solutions. *Chemosphere, 125*, 70–85. https://doi.org/10.1016/j.chemosphere.2014.12.058.

Temkin, M. J., & Pyzhev, V. (1940). Recent modifications to Langmuir isotherms. *Acta Physiologica Chemistry USSR, 12*, 271.

Titirici, M.-M., & Antonietti, M. (2010). Chemistry and materials options of sustainable carbon materials made by

hydrothermal carbonization. *Chemical Society Reviews, 39*(1), 103–116.

Titirici, M.-M., White, R. J., Falco, C., & Sevilla, M. (2012). Black perspectives for a green future: Hydrothermal carbons for environment protection and energy storage. *Energy & Environmental Science, 5*(5), 6796–6822.

Tommaso, G., Chen, W-T., Li, P., Schideman, L., & Zhang, Y. (2015). Chemical characterisation and anaerobic biodegradability of hydrothermal liquefaction aqueous products from mixed-culture wastewater algae. *Bioresource Technology, 178*, 139–146.

UKEA (2019). Environmental Agency, UK. Waste water treatment works: Treatment, monitoring and compliance limits. https://www.gov.uk/government/publications/waste-water-treatment-works-treatment-monitoring-and-compliance-limits/waste-water-treatment-works-treatment-monitoring-and-compliance-limits. Accessed 22 April 2019.

Verma, S., Prasad, B., & Mishra, I. M. (2014). Adsorption kinetics and thermodynamics of COD removal of acid pre-treated petrochemical wastewater by using granular activated carbon. *Separation Science and Technology (Philadelphia), 49*(7), 1067–1075.

Vunain, E., Houndedjihou, D., Monjerezi, M., Muleja, A. A., & Kodom, B. T. (2018). Adsorption, kinetics and equilibrium studies on removal of catechol and resorcinol from aqueous solution using low-cost activated carbon prepared from sunflower (*Helianthus annuus*) seed hull residues. *Water, Soil, & Soil Pollution, 229*, 366.

Weide, T., Brügging, E., & Wetter, C. (2019). Anaerobic and aerobic degradation of wastewater from hydrothermal carbonization (HTC) in a continuous, three-stage and semi-industrial system. *Journal of Environmental Chemical Engineering, 7*, 1–9.

Wignarajah, K., Litwiller, E., Fisher, J., & Hogan, J. (2006). Simulated human feces for testing human waste processing technologies in space systems. In: *36th International conference on environmental systems,* SAE paper no. 2006-01-2180. Norfolk, VA.

Wirth, B., & Mumme, J. (2013). Anaerobic digestion of waste water from hydrothermal carbonization of corn silage. *Applied Bioenergy, 2013*, 1–10. https://doi.org/10.2478/apbi-2013-0001.

Wirth, B., Mumme, J., & Erlach, B. (2012). Anaerobic treatment of wastewater derived from hydrothermal carbonization. In proceedings of the 20th European biomass conference. ETA-Florence Renewable Energies, Florence, Italy.

Wirth, B., Reza, T., & Mumme, J. (2015). Influence of digestion temperature and organic loading rate on the continuous anaerobic treatment of process liquor from hydrothermal carbonization of sewage sludge. *Bioresource Technology, 198*, 215–222. https://doi.org/10.1016/10.1016/j.biortech.2015.09.022.

Xu, R.-K., Xiao, S.-C., Yuan, J.-H., & Zhao, A.-Z. (2011). Adsorption of methyl violet from aqueous solutions by the biochars derived from crop residues. *Bioresource Technology, 102*(22), 10293–10298.

Yakovlev S.V., & Voronov Yu.V. (2002). Sewerage and sewage treatment. M. ed. Construction Association of universities, 512.

Yang, Y., Lin, X., Wei, B., Zhao, Y., & Wang, J. (2014). Evaluation of adsorption potential of bamboo biochar for metal-complex dye: Equilibrium, kinetics and artificial neural network modeling. *International journal of Environmental Science and Technology, 11*(4), 1093–1100. https://doi.org/10.1007/s13762-013-0306-0.

Zdravkov, B. D., Čermák, J. J., Šefara, M., & Josef Janků, J. (2007). Pore classification in the characterization of porous materials: A perspective. *Central European Journal of Chemistry, 5*(2), 385–395. https://doi.org/10.2478/s11532-007-0017-9.